Infrared Ion Dip Spectroscopy of a Noradrenaline Analogue: Hydrogen Bonding in 2-Amino-1-phenylethanol and Its Singly Hydrated Complex

Richard J. Graham, Romano T. Kroemer,[†] Michel Mons,[‡] Evan G. Robertson, Lavina C. Snoek, and John P. Simons*

Physical and Theoretical Chemistry Laboratory, Oxford University, South Parks Road, Oxford, OX1 3QZ, United Kingdom; Department of Chemistry, Queen Mary & Westfield College, University of London, Mile End Road, London E1 4NS, UK; and Service des Photons, Atomes et Molécules, Commissariat à l'Energie Atomique, CEN Saclay, 91191 Gif-sur-Yvette Cedex, France

Received: August 18, 1999

The conformational landscapes of 2-amino-1-phenylethanol and its 1:1 water complexes have been investigated by UV band contour, UV−UV hole-burning, and IR−UV ion dip spectroscopy, coupled with ab initio computation. The two molecular conformers observed are both stabilized by an intramolecular hydrogen bond, located in the folded (gauche) OCCN side chain, which links the proton donor OH group to the terminal amino group and leads to a significant constriction of the side chain. In the dominant 1:1 water complex, the intramolecular hydrogen bond is disrupted by the first water molecule, which inserts between the OH group and the nitrogen atom, to form a cyclic H-bonded structure. The side chain expands significantly in order to accommodate the water molecule within the neighborhood of both the hydroxyl and amino groups.

1. Introduction

Molecular conformation plays a crucial role in the selectivity and function of pharmacologically active molecules. Molecular shape and the interactive forces between the molecule and its nearest neighbors also control molecular recognition processes. These are involved in virtually all aspects of biological function, ranging from neurotransmission and specific drug−receptor interactions to enzyme catalysis. Enzyme function, in its turn, is dependent upon specific interactions between neighboring molecules, bound together at the active site of the enzyme and between the active site and the reactive substrate. It can also be dependent upon the formation of chemically reactive intermediates (transition states) and charge migration within the enzyme−substrate complex.

The factors which control the conformational landscape involve a subtle balance between "through bond" and "through space" interactions within the molecule, and their modification by "nonbonded" interactions with the environment. Hydrogen-bonding interactions are ubiquitous, operating both within the molecules and externally, especially with neighboring water molecules. Together, these interactions determine the molecular architecture, the electronic charge distributions, and the network of pathways for electron and proton transfer within the molecular structure. Their relative influence and the way in which their *cooperative behavior* may control conformational and *supra*molecular structure and the specificity of molecular function remain very unclear.

In the last few years, very powerful strategies have been developed and exploited for exploring and mapping the conformational landscapes of model biomolecules, including neurotransmitters, amino acids, amides, and enzyme inhibitors, and the supramolecular structures of their size-selected hydrates. Ab initio structural computation provides crucially important theoretical input, through which experimental data can be analyzed and interpreted. Theory provides the "à la carte menu" of structural possibilities, and the experiments tell us which ones are actually chosen. The recent development of IR−UV ion dip spectroscopy[1−15] has proved to be an especially elegant tool for the structural assignment of isolated H-bonded molecules, because of its great sensitivity to the local environment of H-bonded chromophores, such as OH or NH_2.

The technique has been used recently to investigate the interplay between inter- and intramolecular H-bonding in hydrated molecular clusters. This issue has been investigated in two molecules with very strong intramolecular H-bonding: tropolone[4−5] and methyl salicylate.[6] Combined spectroscopic measurements and ab initio calculations lead to the conclusion that the presence of up to two bound water molecules does not disrupt the intramolecular H-bond, although there remains some ambiguity in the case of tropolone. The only other published study of hydrated clusters in a molecule with an intramolecular H-bond involves the favored gauche conformer of 2-phenylethyl alcohol, which is stabilized by a weak π-type intramolecular H-bond. The IR spectrum of one of its singly hydrated clusters revealed a structure in which water was inserted between the alcohol group and the aromatic ring, disrupting the weak H-bond.[7]

2-amino-1-phenylethanol (APE) is an analogue of noradrenaline [α-(aminomethyl)-3.4-dihydroxy benzyl alcohol], a molecule which is involved (among other functions) in neuronal communication. It is also related to the ephedra molecules (methyl-substituted APE on the second carbon of the tail), an important class of pharmaceuticals. The flexible side chain allows the possibility of a large number of alternative conformers, and their relative stabilities may be influenced by intramolecular hydrogen-bonded interactions between the neighboring hydroxyl and amino groups. The two groups present both donor and acceptor sites and their presence also introduces the possibility of H-bonded or "nonbonded" interactions between

[†] Queen Mary & Westfield College.
[‡] Commissariat à l'Energie Atomique.

10.1021/jp992903o CCC: $18.00
Published on Web 11/06/1999

the side chain and the aromatic ring: The relative conformer populations, stabilized in the free jet expansion, reflect their relative energies. The APE molecule provides an opportunity to study the interplay of inter- and intramolecular H-bonding, in a case where the functional groups are attached to a flexible framework and bound water molecules may influence the preferred conformation. This important question and its consequences are addressed in the present work.

2. Methodology

The mass-selected resonant two-photon ionization (R2PI) and laser-induced fluorescence (LIF) systems have already been described elsewhere.[16] Briefly, the APE molecules and hydrated complexes were generated in a free jet expansion through a pulsed valve operating at moderate temperature (90 °C) under a typical He stagnation pressure of 3 bar and with room-temperature partial pressure of water when complexes were studied. A commercial sample of APE (Aldrich, racemic mixture) was used without further purification.

UV−UV hole-burn spectra were recorded using two electronically synchronized, Nd:YAG-pumped commercial dye lasers (Lambda Physik FL2002 and Spectra Physics PDL3), operating at 10 Hz and equipped with nonlinear frequency-doubling crystals. The more powerful laser (pulse energy ∼500 μJ) provided the depletion source and was scanned in the region of the $S_1 \leftarrow S_0$ origin transition of APE. The probe laser was delayed by ∼200 ns and successively tuned to the spectral features of interest.

IR−UV ion-dip spectra were recorded with the Lambda-Physik FL2002 used as the probe. IR radiation in the 2.8 μm region was generated by a Continuum laser system, incorporating a $LiNbO_3$ difference frequency generation module at the output of a Nd:YAG-pumped ND6000 dye laser. The IR beam (bandwidth 1 cm^{-1}) had a typical energy of 1.5 mJ per pulse and was mildly focused onto the jet antiparallel to the UV probe laser. The delay between the two was ∼100 ns, which restricted the IR laser depletion to the ground state of the probed species only.

Ab initio calculations on APE and its 1:1 water complexes were performed with the Gaussian suite of programs[17] as an aid to experimental interpretation. Vibrational frequencies were computed using density functional theory at the B3LYP/6-31+G* level, which has been found to give fair agreement with experimental OH frequencies in water-containing H-bonded clusters. HF/6-31G* and MP2/6-31G* level geometry optimizations were also performed to examine relative energies and H-bond lengths.

3. Results

3.1. UV Spectroscopy of the APE Molecule. The mass-selected R2PI spectrum of the APE molecule in the region of its $S_1 \leftarrow S_0$ band origin, recorded in the absence of water (Figure 1a), shows two main bands at 37 685 and 37 693 cm^{-1}, respectively labeled A and B. The small splitting between these features suggests their assignment to the origin bands of two separate conformers, an assignment supported by the UV−UV hole-burning spectra that were generated by tuning the probe laser first onto A and then onto B (Figure 1b). Both hole-burn spectra display strong origin bands accompanied by weaker features, blue-shifted by 36 and 42 cm^{-1}, respectively; these can be ascribed to the excitation of a low-frequency molecular mode in the S_1 state, likely a torsion about the $C_{ipso}-C_\alpha$ bond of the side chain, by comparison with the UV spectroscopy of alkyl benzenes.[18]

3.2. IR Spectroscopy of the APE Molecule. Ion dip IR spectra recorded with the probe laser centred on bands A and B are shown in Figure 2a. Each conformer exhibits an intense band around 3530 cm^{-1} and a much weaker one near 3430 cm^{-1}; see Table 1. The line widths of the strong bands (fwhm 6 cm^{-1}) are greater than the laser line width, and their intensities and frequencies are comparable to the H-bonded OH stretch bands of the 2-phenylethanol−water complexes that were studied previously;[7] on this basis they are assigned to the OH stretch mode. The weaker bands are assigned to the antisymmetric NH stretch modes, as they lie very close to the corresponding band in methylamine (3424 cm^{-1}).[19] The symmetric NH stretch mode, which occurs at 3360 cm^{-1} in methylamine, should be even weaker and could not be observed in our spectra.

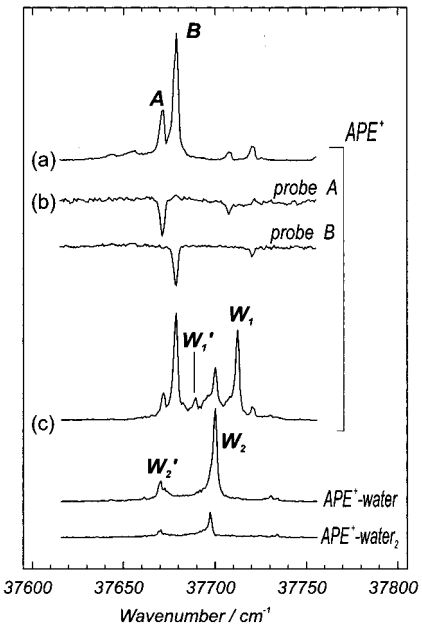

Figure 1. Mass-selected R2PI spectra of APE in the absence of water (a, b) and with water entrained in the carrier gas (c). (b) UV−UV hole-burning spectra of the APE monomer obtained by probing depletion either on band A or B. The mass channel in which the signal was collected in indicated on the right-hand side. Bands assigned to 1:1 complexes are labeled W_1 and W_1', and to 1:2 complexes, W_2 and W_2'.

Comparisons with other systems possessing an OH group clearly show that the observed OH stretch bands cannot be assigned to a free OH group as in ethanol[20] or in the anti conformer of PEAL,[7] each of which has its OH stretch frequency in the 3650−3680 cm^{-1} region. Taking the center of this region as a reference, Table 1 indicates a red shift on the order of 140 cm^{-1} for the OH stretch mode in the two conformers of APE. This appears to be more in line with the frequency of an H-bonded OH group, cf. phenol−water (red shift, 133 cm^{-1}),[8] suggesting its assignment to an OH group acting as a proton donor in an intramolecular H-bond. Two proton-acceptor sites are present in the molecule (the nitrogen atom and the ring), but binding to the π-electron cloud can be excluded, since it generally results in red shifts on the order 30−40 cm^{-1}.[7,9,10] We conclude, therefore, that the OH group is H-bonded to the terminal nitrogen atom on the side chain. When the observed red shift is compared with that in the phenol−ammonia complex (363 cm^{-1}),[11] it is evident that the intramolecular H-bond of the APE molecule is weaker, presumably because of the geometrical constraints exerted by the side chain. We also note that the low intensity and the unperturbed frequency of the NH stretch band (compared with methylamine) both suggest that the amino group is not acting as proton donor, but is consistent with it being a proton acceptor.

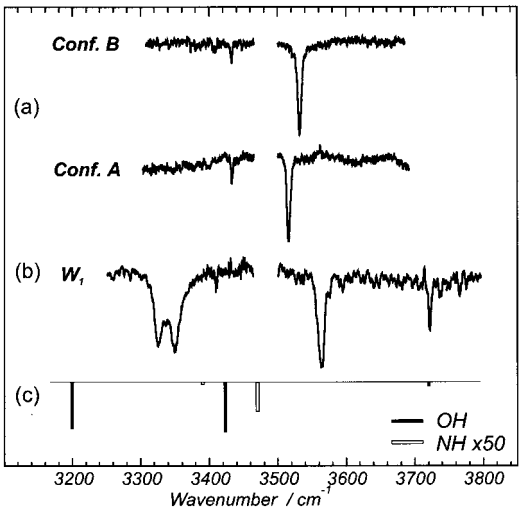

Figure 2. IR ion-dip spectra probing (a) the monomer bands A and B and (b) the complex band W_1. The gap in the IR spectrum of the complex is a consequence of IR absorption by the $LiNbO_3$ crystal. For the sake of comparison, ab initio B3LYP/6-31+G* calculated frequencies of conformer GG−W (Table 3) are also displayed as a stick spectrum (c).

TABLE 1: Experimental and Calculated OH and NH Stretch Frequencies of the Most Stable Conformers of APE

	experimental[a]		ab initio[b]			
	conf A freq/cm^{-1}	conf B freq/cm^{-1}	GG_1 freq/cm^{-1}	int/km mol^{-1}	AG_1 freq/cm^{-1}	int/km mol^{-1}
OH stretch	3516	3532	3514	103	3527	115
NH asym str	3433	3432	3505	4	3502	5
NH sym str			3418	1	3415	0.3

[a] Absolute experimental precision is estimated to be 2 cm^{-1}. [b] B3LYP/6-31+G* results. The frequency scaling factor, 0.976, has been determined using the OH stretches of the water molecule as a benchmark.

Summarizing, these spectroscopic data indicate that two conformers are populated in the jet-cooled environment, one of them (B) being slightly more favored. Both exhibit intramolecular H-bonding, with the OH group acting as a proton donor to the nitrogen atom in the terminal amino group.

3.3. Conformational Landscape of the APE Molecule. As shown by the Newman projections of Figure 3, APE is a chiral molecule, existing in two spectroscopically identical *R* and *S* forms. Taking into account the possible rotation about the $C_\alpha-C_\beta$ bond in the side chain at room temperature, three types of conformer must be considered, which can be classified according to the arrangement [gauche (G) or anti (A)] of their CCCN and OCCN atom chains. Only the AG and GG types bring the OH and NH_2 groups into close proximity, with basically two possibilities for H-bonding, depending on which group acts as a proton donor to the other: $G_1 \equiv OH\cdots N$, $G_2 \equiv NH\cdots O$.

Ab initio calculations conducted for all the possible conformers (HF/6-31G*, with zero-point correction) also suggest that the most stable forms are of AG or GG type, each of which exhibits intramolecular H-bonding. These findings are confirmed by calculations at the MP2/6-311G**//MP2/6-31G* level (see Figure 3). The two most stable conformers are predicted to be those (AG_1 and GG_1) in which the OH group is the proton donor, in full agreement with the IR spectroscopic data. The reversed geometries for H-bonding, where OH acts as the proton acceptor (AG_2, AG_2' and GG_2), are more than 6 kJ mol^{-1} higher in energy, while the first GA form is more than 10 kJ mol^{-1} less stable.

The very small energy difference between the AG_1 and GG_1 forms, on the same order of magnitude as the accuracy of the calculation, makes it necessary to rely on other, more conclusive data to make a firm structural assignment of conformers A and B. To this end, vibrational frequencies have been calculated using the DFT/B3LYP method with a 6-31+G* basis set, which has already given reasonably satisfactory results for similar systems.[12,13] The results (Table 1) show very good agreement for the OH stretch, in both the absolute frequencies and the frequency difference between conformers, provided the most stable conformer B is assigned to the AG_1 structure, and conformer A to GG_1. The absolute frequencies of the NH stretch bands are overpredicted by ca. 70 cm^{-1}. The asymmetric NH stretch bands are predicted to be typically 25 times weaker than the OH bands, in agreement with the spectra of Figure 2. The symmetric NH stretch bands, expected to occur 90 cm^{-1} lower in frequency, are predicted to be even weaker, which is in line with their absence from the experimental spectra.

Additional support for the geometric assignment can be gained from the band contour analysis. Narrow bandwidth fluorescence excitation scans of bands A and B (Figure 4) were analyzed using a cross-correlation fitting procedure.[21,22] Table 2 and Figure 4 present the results of such an optimization, together with the ab initio predictions for the GG_1 and AG_1 forms. The excellent agreement found between the experimental and predicted structures, assuming that the most stable conformer B has a AG_1 geometry, confirms the provisional assignment.[23]

3.4. UV and IR Spectroscopy of the APE−Water Complex. When water was present in the carrier gas, the R2PI spectrum in the region of the $S_1 \leftarrow S_0$ monomer band origin, obtained by monitoring the APE^+ mass channel, exhibited two additional features: a main band labeled W_1 in Figure 3 (shifted 33 cm^{-1} relative to band B) and a minor band W_1' (shifted 10 cm^{-1} relative to band B). Spectra recorded with different delays between the opening of the valve and the arrival of the laser pulse show that these features appear significantly later in the expansion than the cold monomers. This observation suggests that the features might be associated with hydrated complexes of APE, although there is no hint of their presence in the $[APE-(water)_1]^+$ mass channel. Instead, two other features labeled W_2 and W_2' can be detected, each of which appear even later than bands W_1 and W_1'. This leads to the conclusion that W_1, W_1' and W_2, W_2' may be assigned to, respectively, singly and doubly hydrated clusters that tend to undergo highly efficient fragmentation following photoionization. Such behavior is generally observed when the neutral species and the complex ion have very different equilibrium geometries, e.g. the π-bonded benzene−water[9] or 1-methylindole−water[13] complexes. The implications will be discussed later in connection with the structure of the APE−water complexes.

The IR−UV ion dip spectrum of the most intense 1:1 APE−water complex feature, band W_1, is shown in Figure 2c. It exhibits three intense features (Table 3) readily ascribed to the OH oscillators of a 1:1 water complex. The most red-shifted feature is actually a doublet of two broad (fwhm 20 cm^{-1}) bands of similar intensities. Such a red shift of more than 300 cm^{-1}, when compared to our previous free OH reference, is reminiscent of the phenol−ammonia system and suggests tentative assignment to a strong OH→N bond. The nature of the doublet structure will be discussed later. The broad (fwhm, 11 cm^{-1}) and intense band in the intermediate region (3562 cm^{-1}) corresponds well to the expectation for an OH→O bond, and the narrow, weak band at 3722 cm^{-1} is typical of the free OH

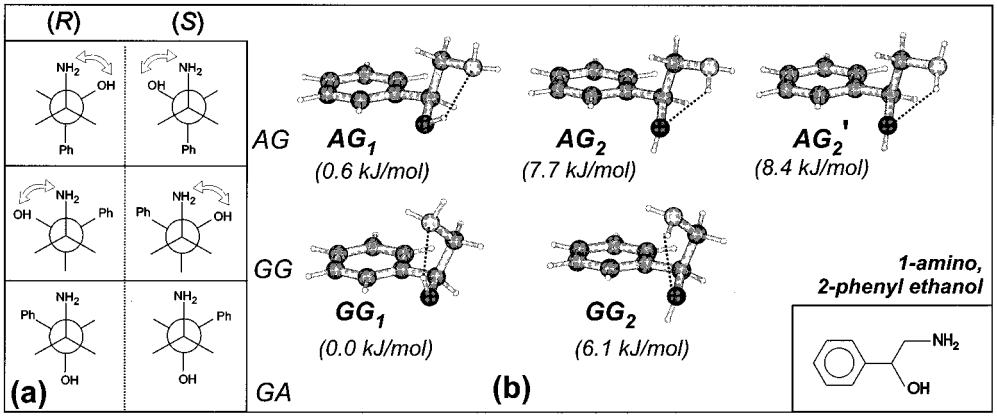

Figure 3. Conformations of APE. (a) Newman representations of the APE molecule, showing the possible occurrence of H-bonds (arrows); (b) ab initio MP2/6-311G**//MP2/6-31G* predictions with their relative energies, including a zero-point correction taken at the HF/6-31G* level. The conformers are labeled according to the arrangement of the side chain with respect to CCCN (gauche/anti) and OCCN (gauche/anti). The subscript indicates the direction of the H-bond.

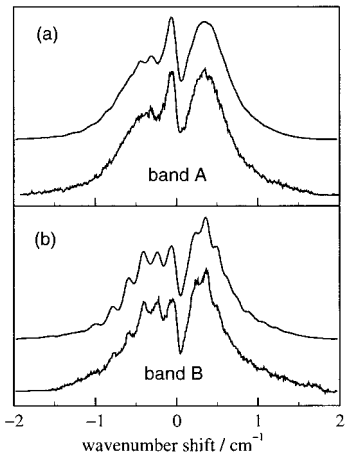

Figure 4. Experimental and simulated rotational band contours for the two $S_1 \leftarrow S_0$ origin bands of APE: (a) band A and (b) band B. Lower traces: experimental LIF spectra. Upper traces: optimized simulations using the data from Table 2, $T_{rot} = 2.5$ K and laser line width = 0.110 cm^{-1} for (a) and 0.093 cm^{-1} for (b).

TABLE 2: Fitted Molecular Parameters and Ab Initio Predictions for Conformers of APE

	experimental		ab initio structures	
	band A	band B	GG_1	AG_1
$(A-\bar{B})''$ [a]/cm^{-1}	0.0574	0.0809	0.0564	0.0805
$\bar{B}''$ [a]/cm^{-1}	0.0289	0.0244	0.0289	0.0245
$(B-C)''$ [a]/cm^{-1}	0.0025	0.0032	0.0027	0.0028
$\mu_a^2:\mu_b^2:\mu_c^2$ [b]	50:48:2	41:55:4	70:29:1	72:28:0

[a] Ab initio values from the MP2/6-31G* geometry. [b] Ab initio values from CIS/6-31G* calculations.

stretch of a single donor water molecule.[7,9] These basic assignments suggest that the nitrogen atom of APE, which still acts as a proton acceptor, is now involved in a much stronger H bond with an OH group. From the results on the monomer, which have shown that the geometrical constraint exerted by the side chain forbids a strong intramolecular H-bond, one can draw the conclusion that the donor hydroxyl group is associated with the water molecule. The two remaining OH bands are assigned to the OH group of APE and to the free OH group of water. It is quite striking that the OH stretch of the APE complex is actually *less* red-shifted in the complex than in the free molecule. This implies disruption of the intramolecular H-bond, in order to form a bridged structure in which the water links the OH group and the N atom of APE. The weak band at 3409 cm^{-1}, red-shifted by 23 cm^{-1} relative to the weak band of the monomer, is assigned to the solvation-perturbed asymmetric NH stretch mode.

TABLE 3: Experimental Vibrational Frequencies for the W_1 Complex and Calculated OH and NH Stretch Frequencies for the Two Most Stable 1:1 Complexes of APE with Water

experimental[a]		ab initio			
complex W_1 freq/cm^{-1}	assignment	GG−W freq/cm^{-1}	int/km mol^{-1}	AG−W freq/cm^{-1}	int/km mol^{-1}
3349	$OH_{water} \rightarrow N_{APE}$	3197	559	3221	590
3562	$OH_{APE} \rightarrow O_{water}$	3424	595	3444	851
3722	free OH_{water}	3719	51	3722	69
3409	APE NH_2 asym	3471	7	3463	4
3325	APE NH_2 sym	3391	0.5	3383	0.1

[a] Absolute experimental precision is estimated to be 2 cm^{-1}. [b] B3LYP/6-31+G* results. The frequency scaling factor, 0.976, has been determined using the OH stretches of the water molecule as a benchmark.

These assignments are supported by MP2/6-31G*//HF/6-31G* ab initio calculations conducted on the 1:1 complex. Assuming either an AG_1 or GG_1 geometry for the monomer, the most stable hydrated structures are those in which the water inserts between the donor and acceptor sites of the molecule (structures AG−W and GG−W of Figure 5a), disrupting the intramolecular H-bond of the corresponding monomer. GG−W, the structure based on the GG_1 monomer, is predicted to be 5.8 kJ mol^{-1} more stable than AG−W, using MP2/6-31G* energies with B3LYP/6-31+G* zero-point corrections, which favors the GG−W assignment. Unfortunately, the OH and NH stretch frequencies calculated for the AG−W and GG−W complexes using the DFT/B3LYP method with a 6-31+G* basis set are very similar (Table 3). A stick spectrum of GG−W is displayed in Figure 2 for comparison with experiment. The agreement is far from perfect and, from this comparison alone, it would not be possible to assign the form responsible for the complex band W_1. Some of the trends are reproduced satisfactorily, e.g. the relative intensities, although the frequencies of OH oscillators involved in H-bonds are systematically predicted to be too red-shifted. This is often the case for DFT calculations on cyclic H-bonded structures.[7,9,13] The predictions that the asymmetric NH stretch should still be weak, and red-shifted by 35 cm^{-1} relative to the corresponding monomer band, are in fair agreement with observation. The symmetric NH stretch is calculated to be red-shifted by 80 cm^{-1} relative to the asymmetric NH mode and might therefore be expected to appear

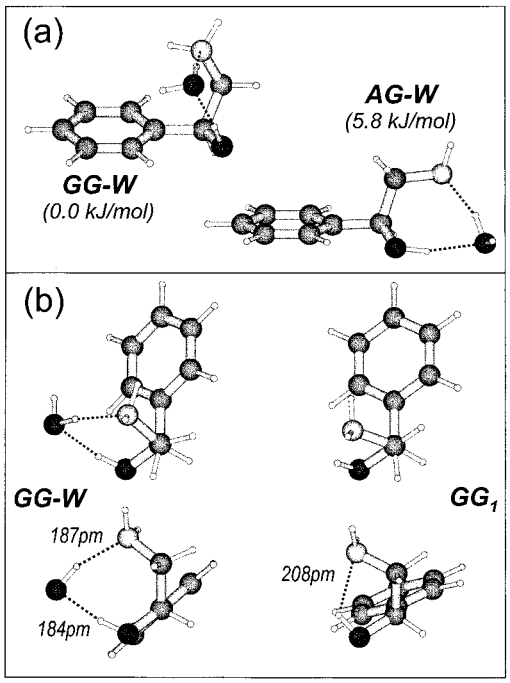

Figure 5. Ab initio (MP2/6-31G*) predictions of the 1:1 APE−water complexes. (a) The most stable structures for water binding to the two lowest energy conformations, labeled GG−W and AG−W; relative energies at the MP2/6-31* level, including B3LYP/6-31G* zero-point corrections, are shown underneath. (b) Detailed comparison of the GG−W hydrate with its corresponding GG_1 monomer.

at around 3329 cm^{-1}. This value lies between the center of the intense doublet and its lower frequency component. It suggests an assignment of the doublet to a Fermi resonance between the highly red-shifted OH→N water mode and the symmetric NH stretch mode of APE. The similar intensities suggest that the unperturbed levels are very close together, and are consistent with a Fermi resonance between a nearly dark state (NH sym) and a bright state (OH→N). Under these circumstances, the splitting (25 cm^{-1}) indicates the strength of the coupling. A similar intensity enhancement of the bending overtone of water in $Br^-(H_2O)$ was also ascribed to a Fermi resonance with the red-shifted OH stretch band.[14]

4. Discussion

4.1. Molecular Conformers. Experiment and calculations both conclude that those conformers having an intramolecular H-bond are the most stable, with the OH group acting as a donor to the strong nitrogen acceptor. This is in line with the gas-phase structure of the water−ammonia complex,[25] but the ab initio calculations also show that the H-bond in both the AG_1 and GG_1 conformers is not as strong. At the MP2/6-31G* level, which takes into account the dispersion forces, the H···N distance is longer (208 pm) than is found for the water−ammonia complex at this level (199 pm) and the small bond angle (119°) evokes a highly distorted bond. Despite the nonoptimal character of the intramolecular bond, it has a considerable effect on the geometry of the side chain, acting against the constraint exerted by the sp^3 character of its carbon atoms. A close examination reveals a constriction, illustrated by the reduced OCCN dihedral angle (52°) when compared with the 60° angle expected in the absence of any H-bond interaction.

This constriction of the OCCN side chain also plays a role in the relative energies of several conformers and therefore affects their relative abundance. A comparison of conformational populations in phenylethylamine (PEA) and APE illustrates the point. The counterparts of both the AG_1 and GG_1 APE conformers are observed in PEA. The latter one, the gauche form of PEA, is by far the most abundant species, since it is stabilized by a π-type H-bond between one of the amine hydrogens and the ring.[15] In APE, however, the trend is reversed. The constriction due to the intramolecular OH···N attraction pulls the terminal NH_2 group in GG_1 away from the ring (see Figure 5b), which greatly reduces the strength of the π H-bond. Deprived of this additional stabilization, the GG_1 form is no longer the preferred conformer.

4.2. APE−Water Complex. The singly hydrated complex of APE exhibits a cyclic H-bonded structure. This is energetically favorable since the nonoptimal H-bond of the monomer is replaced by two more conventional H-bonds. The intermolecular OH_{APE}···O and OH_{water}···N distances are calculated to be 184 and 187 pm, respectively, at the MP2/6-31G* level, and the two H bonds are close to linear, with angles calculated to be 169° and 161°, respectively, in GG−W. The extra degrees of freedom in the hydrated system, together with the flexibility of the side chain, facilitate this optimal geometrical arrangement. The distortion of the tail in GG_1 is well-depicted in Figure 5b, where the monomer geometry is also shown for comparison. The OCCN dihedral angle is now 78°, which is greater than the 60° expected in an unperturbed alkyl chain. This indicates an expansion of the side chain, also illustrated by the N···O distance of 310 pm compared to 277 pm in the GG_1 molecular conformer. Figuratively speaking, the side chain of APE acts like a pair of pliers, which open up to grip an OH of the water molecule.

As was the case with the monomer, distortion of the side chain also has consequences for the relative abundance of the two complex conformations. In the GG−W conformation, the terminal amino group is pushed toward the ring (Figure 5b), thus energetically favoring this form by the enhancement of the π H-bond. This cooperative effect could well explain the observation of only one prominent APE−water complex band, in contrast with two for the monomer. On this unique basis, since the IR data do not allow us to discern the host geometry within the complex, the W_1 band of Figure 1 is assigned to the GG−W complex. The substantial reduction in the relative population of the bare GG_1 conformer (peak A) displayed in the R2PI spectra (Figure 1c compared with Figure la) is also consistent with a selective depletion of the GG_1 conformer through hydration.

The IR bands in the spectra of Figure 2 show great variability in line width. Although power broadening may contribute to the measured line widths,[15] some trends are clear. In particular, the H-bonded oscillators exhibit larger bandwidths than the free oscillators (fwhm ca. 20 cm^{-1} for the OH_{water}→N band of W_1, ca. 11 cm^{-1} for the OH_{APE}→O band of W_1 and ca. 6 cm^{-1} for the OH_{APE}→N bands of conformers A and B, compared to <3 cm^{-1} for the free OH and NH_{asym} modes). These line widths reflect the IVR rates in the vibrationally excited levels, but the similar energy range of these levels, and therefore the similar state density of the isoergic bath, suggests that the line widths are real indicators of the actual coupling between the excited modes and the corresponding bath. The present IR spectra clearly reveal selectivity in this coupling. The free oscillators are weakly coupled to the rest of the molecule, whereas those oscillators involved in a H-bonding network are much more strongly coupled, in particular because of the quasidegeneracy of the frequencies of all the H-bonded OH oscillators. This is supported by the vibrational mode descriptions obtained from the ab initio calculations, which frequently show a significant

distribution of the motion along the H-bonded network. It is also apparent that the most red-shifted bands are also the broadest. Since the red shift is a good indicator of the perturbation induced by the H-bond and therefore of the bond strength, this correlation implies an increase in coupling with increasing H-bond strength. An additional consequence of this correlation is that the broadest bands will tend to be the most intense, since bond strength is generally linked to IR band intensity through bond polarisation. The $OH_{water} \rightarrow N$ oscillator of W_1 is obviously the best example. Although the relationship is not straightforward, it is actually a general feature of the IR spectra which explains why bands having overall intensities which differ by more than 2 orders of magnitude actually cause ion depletions which differ by less than 1 order of magnitude. This characteristic allows bands with very different intensities to be observed in the same spectrum, without the need for large variations in the dynamic range.

Finally, the 100% fragmentation efficiency of the ionized APE−water complex deserves some comment. Such behavior might appear surprising at first glance, because water is attached via two H-bonds and no great changes in the intermolecular geometry following photoionization would be expected, providing that the charge remains localized on the ring. Earlier studies on phenylethylamine, however, reveal that important geometry changes occur in the monomer upon photoionization, due to strong coupling between two closely lying ionic states associated with charge localization either on the ring or on the amino group.[26] In the similar case of APE, such a (partial) charge transfer is also expected following ionization, resulting in a substantial change in molecular geometry between neutral and ionic states. Photoionization, obeying Franck−Condon rules, leaves the molecular cation in highly excited vibrational states. In addition to this, the 1:1 hydrate geometry with the water molecule as donor to the nitrogen atom in the neutral complex is repulsive in the ion. The combination of these two factors leads to rapid fragmentation. A similar explanation holds for the phenylethylamine−water complex, where the water molecule is also bound as a proton donor to the nitrogen atom and which has been reported to fragment with a similar high efficiency.[27]

5. Conclusion

The present study shows how the local information derived from IR spectroscopy provides valuable insights into the overall geometry of nonrigid molecular conformers and their hydrated complexes. Assignments can be further refined experimentally, using band contour spectroscopy, and theoretically, using high-level ab initio computation. The results on the monomer, which are probably also relevant for the description of the simpler molecule, 1-aminoethanol, as well as the more complex neurotransmitter, noradrenaline, show that intramolecular H-bonding controls both the conformational structure and the relative conformational abundance. The theoretical study confirms the H-bonded structure revealed experimentally, and in particular, the disruption of the intramolecular H-bond by the first bound water molecule. It also reveals the key role of side chain flexibility and cooperative effects in this neurotransmitter analogue.

The present system may also be viewed as a model for the biological process of "docking", with the amino group playing the role of a docking molecule and the rest of the molecule acting as the substrate. The limited tail flexibility of the free conformer models the constraints arising from the overall structure of the docking−substrate complex. The behavior of the hydrate may also illustrate the role played by interfacial water molecules in the docking process. By adding extra degrees of freedom to the system in the critical region of the molecular anchors, they allow optimization of the bond strength, without preventing subsequent processes like proton transfer between the docking molecule and its substrate, because of the continuous chain of H-bonds.

Acknowledgments. We are grateful to the EPSRC for grant support and for the provision of a visiting fellowship (to M.M.) and to the Leverhulme Trust for postdoctoral support (E.G.R.). We thank the Laser Support Facility at the Rutherford Appleton Laboratories for the loan of the IR laser system and especially Dr. M. Towrie for his assistance with laser installation and maintenance. We also much appreciated receiving a prepublication copy of ref 13, from Prof. Timothy Zwier.

References and Notes

(1) Page, R. H.; Shen, Y. R.; Lee, Y. L. *J. Chem. Phys.* **1988**, *88*, 4621−4636.

(2) Tanabe, S.; Ebata, T.; Fujii, M.; Mikami, N. *Chem. Phys. Lett.* **1993**, *215*, 347−352.

(3) Pribble, R. N.; Zwier, T. S. *Science* **1994**, *265*, 75−79.

(4) Frost, R. K.; Hagemeister, F. C.; Arrington, C. A.; Schleppenbach, D.; Zwier, T. S. *J. Chem. Phys.* **1996**, *105*, 2605−2617.

(5) Mitsuzuka, A.; Fujii, A.; Ebata, T.; Mikami, N. *J. Chem. Phys.* **1996**, *105*, 2618−2627.

(6) Mitsuzuka, A.; Fujii, A.; Ebata, T.; Mikami, N. *J. Phys. Chem. A* **1998**, *102*, 9779−9784.

(7) Mons, M.; Robertson, E. G.; Snoek, L. C.; Simons, J. P. *Chem. Phys. Lett.* **1999**, *310*, 423−432.

(8) Watanabe, T.; Ebata, T.; Tanabe, S.; Mikami, N. *J. Chem. Phys.* **1996**, *105*, 408−419.

(9) Fredericks, S. Y.; Jordan, K. D.; Zwier, T. S. *J. Phys. Chem.* **1996**, *100*, 7810−7821 and references therein.

(10) Pribble, R. N.; Hagemeister, F. C.; Zwier, T. S. *J. Chem. Phys.* **1997**, *106*, 2145−2157.

(11) Iwasaki, A.; Fujii, A.; Watanabe, T.; Ebata, T.; Mikami, N. *J. Phys. Chem.* **1996**, *100*, 16053−16057.

(12) Gruenloh, C. J.; Carney, J. R.; Hagemeister, F. C.; Arrington, C. A.; Zwier, T. S. *J. Chem. Phys.* **1998**, *109*, 6601−6613.

(13) Carney, J. R.; Zwier, T. S. *J. Phys. Chem. A.* Submitted.

(14) Ayotte, P.; Weddle, G. H.; Kim, J.; Johnson, M. A. *J. Am. Chem. Soc.* **1998**, *120*, 12361−12362.

(15) Spangenberg, D.; Imhof, P.; Roth, W.; Janzen, Ch.; Kleinermanns, K. *J. Phys. Chem. A* **1999**, *103*, 5918−5924.

(16) Dickinson, J. A.; Hockridge, M. R.; Kroemer, R. T.; Robertson, E. G.; Simons, J. P.; McCombie, J.; Walker, M. *J. Am. Chem. Soc.* **1998**, *120*, 2622−2632.

(17) Frisch, M. J.; Trucks, G. W.; Schlegel, H. B.; Gill, P. M. W.; Johnson, B. G.; Robb, M. A.; Cheeseman, J. R.; Keith, T.; Petersson, G. A.; Montgomery, J. A.; Raghavachari, K.; Al-Laham, M. A.; Zakrzewski, V. G.; Ortiz, J. V.; Foresman, B.; Cioslowski, J.; Stefanov, B. B.; Nanayakkara, A.; Challacombe, M.; Peng, C. Y.; Ayala, P. Y.; Chen, W.; Wong, M. W.; Andres, J. L.; Replogle, E. S.; Gomperts, R.; Martin, R. L.; Fox, D. J.; Binkley, J. S.; Defrees, D. J.; Baker, J.; Stewart, J. P.; Head-Gordon, M.; Gonzalez, C. and Pople, J. A. Gaussian 94, Revision C.3; Gaussian, Inc., Pittsburgh PA, 1995.

(18) Dickinson, J. A.; Joireman, P. W.; Kroemer, R. T.; Robertson, E. G.; Simons, J. P. *J. Chem. Soc., Faraday Trans.* **1997**, *93*, 1467−1472.

(19) Hamada, Y.; Tanaka, N.; Sugawara, Y.; Hirakawa, A. Y.; Tsuboi, M.; Kato, S.; Morokuma, K. *J. Mol. Spectrosc.* **1982**, *96*, 313−330.

(20) Fang, H. L.; Sworfford, R. L. *Chem. Phys. Lett.* **1984**, *105*, 5−11 and references therein.

(21) Elkes, J. M. F.; Robertson, E. G.; Simons, J. P.; McCombie, J.; Walker, M. *Phys. Chem. Commun.* **1998**, *3*.

(22) Hockridge, M. R.; Knight, S. M.; Robertson, E. G.; Simons, J. P.; McCombie, J.; Walker, M. *PCCP* **1999**, *1*, 407−413.

(23) The orientation of the transition moment relative to the inertial axes, which controls the $\mu_a^2:\mu_b^2:\mu_c^2$ hybridization parameters, is only poorly predicted by the CIS/6-31G* calculations of the excited state, in marked contrast to its success for several very similar molecules:[24] the error in the orientation amounts to 12° for A and to 19° for B.

(24) Kroemer, R. T.; Liedl, K. R.; Dickinson, J. A.; Robertson, E. G.; Simons, J. P.; Borst, D. R.; Pratt, D. W. *J. Am. Chem. Soc.* **1998**, *120*, 12573−12582.

(25) Herbine, P.; Dyke, T. R. *J. Chem. Phys.* **1985**, *83*, 3768−3774.

(26) Lehrer, F. Ph.D. Thesis, Technical University of Munich, 1997.

(27) Hockridge, M. R.; Robertson, E. G. *J. Phys. Chem. A* **1999**, *103*, 3618−3628.